RSC Advances

ROYAL SOCIETY OF CHEMISTRY

www.rsc.org/advances

Cite this: DOI: 10.1039/c0xx00000x

www.rsc.org/xxxxxx

ARTICLE TYPE

Construction of hydrated tungsten trioxide nanosheet films for efficient electrochromic performance

Haizeng Li,[a] Jinmin Wang,[b] Guoying Shi,[d] Hongzhi Wang,*[a] Qinghong Zhang[c] and Yaogang Li*[c]

Received (in XXX, XXX) Xth XXXXXXXXX 20XX, Accepted Xth XXXXXXXXX 20XX

DOI: 10.1039/b000000x

Tungsten trioxide hydrate ($WO_3 \cdot 0.33H_2O$) films with different morphologies were directly grown on fluorine doped tin oxide (FTO) substrate. With the directing effect of seed layer, $WO_3 \cdot 0.33H_2O$ thin films composed of nanosheets structures could be selectively synthesized. The effect of urea was also discussed in this paper. The crystal-seed-assisted film grown with urea as a capping agent exhibits efficient electrochromic performances.

Introduction

Construction of functional films with large surface area and desired morphologies is an important prerequisite for large scale electronic and optoelectronic applications with improved performance.[1-3] Tungsten oxide (hydrate) film, an important functional coating, has attracted extensive attention due to its wide-ranging applications in gas sensor,[4] photoelectrochemical (PEC) device,[5] dye-sensitized solar cell[6] and electrochromic device (ECD).[7-9] More recently, renewed research interest in tungsten oxide (WO_3) is sparked by the development of its electrochromic (EC) applications.[10,11]

Electrochromism is the reversible and persistent optical change that is associated with an electrochemically induced oxidation–reduction reaction after applying an appropriate potential on the electrochemical active materials.[12] As mentioned above, electrochromism has attracted immense attention and is considered to be one of the most promising candidates for energy-saving smart (ESS) windows. WO_3 (hydrate), a traditional EC material, exhibits fairly good optical modulation and high cycle stability. Therefore, a lot of research has been conducted to synthesize WO_3 (hydrate) films for electrochromic devices.[7]

In the past decades, many electrochromic (EC) studies of WO_3 have focused on amorphous WO_3 (a-WO_3) films because of their fast switching responses and high coloration efficiencies (CEs).[13,14] However, a-WO_3 thin films also suffer from poor electrochromic stability due to their poor chemical stability and non-compact structure.[8,15] Crystalline WO_3 films have better electrochemical stabilities, but leading to slower switching responses and lower CEs.[12,16] Thus, designing nanocrystalline WO_3 films is the key to obtain materials with fast insertion kinetics, enhanced durability, and superior performance.[17,18] High-performance nanoscale WO_3 (hydrate) films have been constructed on a transparent conductive substrate via various techniques, such as sol–gel reaction method,[19] sputtering,[20] anodic growth method[21] and hydrothermal approach.[22] The hydrothermal approach stands out to be a facile, dominant tool for the synthesis of crystalline oxides, which is promising for the construction of WO_3 (hydrate) films because of its advantages, including suitability for large-scale production, low reaction temperatures and cost-effectiveness. [23-25]

With the dramatic development of graphene, two-dimensional (2D) materials have received increasing attention in recent years, owing to their unique electronic and optical properties.[26,27] 2D materials are considered one of the most promising electrode materials not only due to their large surface area, high electrical conductivity,[28] but also because the 2D materials can be used as building blocks to construct complex nanostructures.[29] Thus, 2D WO_3 (hydrate) nanosheet, with high surface ratio and permeable channels, could be a promising building block for constructing EC electrode.[7]

Recently, WO_3 (hydrate) nanosheets are mainly obtained via exfoliation method.[30,31] However, the amount of the products and long cycle of exfoliation process hinders the research and applications of the exfoliation technique. Moreover, the current construction of WO_3 (hydrate) nanosheet electrode is usually by layer-by-layer technique, which is inconvenience in preparing large area nanosheet electrodes. Moreover, the layer-by-layer tight stacking in their thin film form will inevitably diminish the interlayer space between nanosheets, which could significantly hinder the electrolyte ion diffusion.[32] In contrast, hydrothermal approach can not only synthesize 2D WO_3 nanosheets, but also construct complex nanostructures in "one pot" route.[7] Herein, we make an attempt to construct a WO_3 (hydrate) nanosheet film to resolve the aforementioned issues. The constructed hydrated tungsten trioxide nanosheet films may prove to be a promising electrode for electrochromism due to their unique features including high optical transparency and highly porous space among the nanosheets.

Results and discussion

Structure and morphology analysis

Many factors can affect the formation and crystal growth of hydrothermal products, including the seed layer (SL), capping agent, solvent system, temperature, and reaction time. In this report, with the aim of obtaining a clear understanding of the effect of SL and urea on constructing WO_3 (hydrate) films, we compared the samples prepared with/without SL and urea.

SL plays an important role in hydrothermal process.[33,34] To investigate the influence of the SL on the structure and morphology of as-synthesized film, bare FTO substrate without SL was compared. Fig. 1(a) shows the X-ray powder diffraction (XRD) patterns of the bare FTO glass and the as-prepared films grown with and without a WO_3 seed layer deposited on an FTO-coated glass substrate. The XRD pattern of the FTO glass can be clearly indexed to tin oxide (JCPDS Card No. 70-4176), all peaks of the as-prepared films can be well indexed to the orthorhombic phase of $WO_3 \cdot 0.33H_2O$ (JCPDS Card No. 54-1012). The as-prepared films have the same crystalline structure since all diffraction peaks appear at the same positions. However, the relative peak intensity for crystalline plane of (020) of the film grown without SL prepared in advance is different from the one with SL, indicating a different preferred growing direction due to the directing effect of the SL.

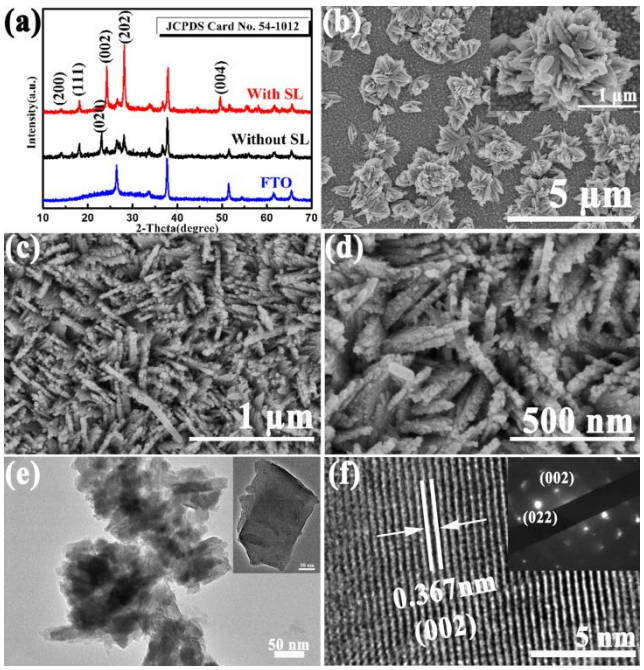

Fig. 1 Characterization of as-prepared $WO_3 \cdot 0.33H_2O$ electrodes. (a) XRD pattern of the as-prepared $WO_3 \cdot 0.33H_2O$ electrodes. (b) FE-SEM images of the $WO_3 \cdot 0.33H_2O$ electrode without SL prepared in advance. The inset is a partially enlarged view. (c, d) FE-SEM images of $WO_3 \cdot 0.33H_2O$ electrode with SL prepared in advance. (e) TEM image of $WO_3 \cdot 0.33H_2O$ electrode with SL. The inset shows an individual $WO_3 \cdot 0.33H_2O$ nanosheet. (f) HRTEM image of $WO_3 \cdot 0.33H_2O$ nanosheet and the corresponding SAED pattern (inset).

The morphologies of as-prepared $WO_3 \cdot 0.33H_2O$ electrode without SL prepared in advance are shown in Fig. 1(b). It can be seen that flower-like nanorod bundles spreading on the surface of FTO with diameter of ~1.5 μm were synthesized. In contrast, the morphologies of the as-prepared $WO_3 \cdot 0.33H_2O$ electrode exhibit drastic differences when the FTO substrates were coated with SL before hydrothermal process, as shown in the SEM and TEM images. Fig. 1(c,d) shows that the nanosheets have a coarse surface, making a larger surface area available for reactions in electrochemical processes. The nanosheet with a thickness of ~35 nm grew disorderly on the substrate, forming a quite rough surface. It is because the drastic differences in morphologies between the electrodes prepared with and without SL, that the transmittance of the electrode prepared with SL is ~30% higher than that of the electrode prepared without SL in the entire visible light region (see Fig. S1 in ESI). Fig. 1(e) shows the $WO_3 \cdot 0.33H_2O$ nanosheets scraped from the substrate. The inset of Fig. 1(e) shows the representative TEM image of an individual nanosheet, indicating that the lateral size of the nanosheet is ~300nm. Clear lattice fringes correspond to the d-spacing of (002) planes with lattice spacing of 0.367 nm are shown in Fig. 1(f), further indicating its single-crystal quality, which is in good agreement with Fig. 1(a). The inset of Fig. 1(f) shows the SAED pattern of the nanosheet and its single-crystal quality could be proved by the regular diffraction spots.

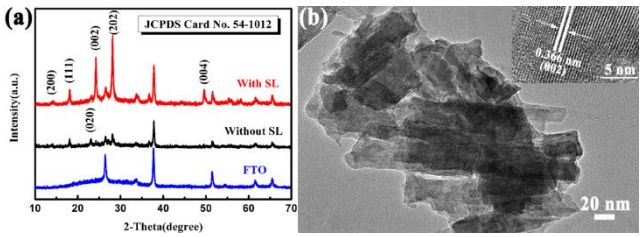

Fig. 2 Characterization of as-prepared $WO_3 \cdot 0.33H_2O$ electrode prepared without urea. (a) XRD pattern of the as-prepared $WO_3 \cdot 0.33H_2O$ electrode. (b) TEM image of the as-prepared $WO_3 \cdot 0.33H_2O$ and the corresponding HRTEM image (inset).

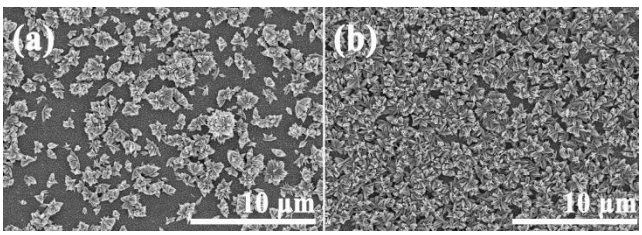

Fig. 3 FE-SEM images of the as-prepared $WO_3 \cdot 0.33H_2O$ electrode (without SL) prepared with and without urea. (a) The as-prepared $WO_3 \cdot 0.33H_2O$ electrode prepared with urea. (b) The as-prepared $WO_3 \cdot 0.33H_2O$ electrode prepared without urea.

For comparison, precursor solution without urea was compared as well. Corresponding XRD patterns are shown in Fig. 2(a), which indicate that there is no change in the phase of the as-prepared electrodes without urea used for hydrothermal process. The TEM image shown in Fig. 2(b) exhibits that the electrodes prepared with SL are still constructed by nanosheet. HRTEM image is shown in the inset of Fig. 2(b). Clear lattice fringes correspond to the d-spacing of (002) planes with lattice spacing of 0.366 nm, indicating single-crystal quality of the $WO_3 \cdot 0.33H_2O$ nanosheets, which is in good agreement with the XRD result (Fig. 2(a)). Morphologies of the as-synthesized film are shown in Fig. 3. It can be seen that there are numerous empty surface regions that showed no $WO_3 \cdot 0.33H_2O$ growth when the electrode prepared with urea (without SL) (Fig. 3(a)). In contrast, the $WO_3 \cdot 0.33H_2O$ flower-like nanorod bundles almost spread on the whole electrode prepared without urea (without SL) (Fig. 3(b)). This is consistent with our previous report,[9] the addition of urea could decrease the number of nucleation sites for the growth of WO_3 nanocrystal. Besides, the addition of urea could also facilitate the formation of hollow structures and improve the monodispersity.[35] Moreover, the presence of urea can also promote an oriented attachment growth, which means that the widths of the nanosheets will be increased.[9] Thus, the sample prepared with urea could get larger

lateral sizes. The average lateral size of the nanosheets prepared with urea is 207.5 nm, while that of sample prepared without urea is 172.2 nm (See Fig. S2). The larger nanosheets could make the sample prepared with urea have a higher surface area, which can be proved by the qualitative measures of electrochemical available surface (See Fig. S3). This change could obviously affect their electrochromic performance.

Electrochromic properties

The EC properties of the as-prepared $WO_3 \cdot 0.33H_2O$ electrodes (with SL) prepared with and without urea were measured at room temperature using the CHI-760D electrochemical work station via a three-electrode configuration in 1 M lithium perchlorate ($LiClO_4$)-propylene carbonate (PC) electrolyte solution, employing the as-prepared electrode as working electrode and a Pt wire (0.5 mm diameter) as the counter electrode together with an Ag/AgCl (3 M KCl) reference electrode. The UV-vis transmittance spectra of the $WO_3 \cdot 0.33H_2O$ electrode prepared with urea in the bleached and colored states were measured at 1.0 V and -1.0 V, respectively, for 60 s (Fig. 4). Generally, when the $WO_3 \cdot 0.33H_2O$ electrodes were cathodically polarized, they had a very uniform blue color, which intensified with increasing cathodic potential. When the blue electrodes were anodically polarized, they were bleached and transparent (inset in Fig. 4). It can be seen from Fig. 4 that the transmittance of the film prepared with urea at 632.8 nm is up to be ~70% when bleached. In addition to the high transmittance of the bleached state, the film has a fairly high modulation range when colored. The modulation range of the film at 632.8 nm is calculated to be 67.1 %, which is 11.3 percent higher than that of the $WO_3 \cdot 0.33H_2O$ film prepared without urea (see Fig. S4 in ESI) and approximately equal to the result in previous report when colored at -3.0 V for 60 s.[8] This good electrochromic performance can be attributed to the high surface ratio and permeable channels of 2D nanosheets structures.

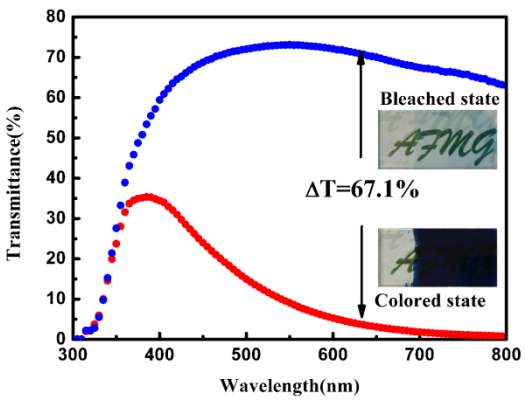

Fig. 4 UV-vis transmittance spectra of the $WO_3 \cdot 0.33H_2O$ electrode prepared with urea at its colored and bleached state.

The assessment of the coloration−bleaching kinetics are vital for the evaluation of optical and electronic properties of the films.[36,37] Therefore, in situ transmittance changes measured at an optical wavelength of 632.8 nm were carried out during the chronoamperometric (CA) measurements (Fig. 5). The coloration and bleaching times are defined as the time required for 90 % change in the entire transmittance modulation. The data shown in Table 1 exhibits the coloration and bleaching times under different applied potentials, which are all faster than those of previous reports.[38,39] The experimental data indicate that there are only modest variation in coloration and bleaching times between the electrode prepared with urea and without urea. The reason is that the larger transmittance variation will take longer color switching time at the same switching speed and the electrode prepared with urea has a larger transmittance variation.

Coloration efficiency (CE), which is defined as the change in optical density (ΔOD) per unit of charge (ΔQ) intercalated into the EC layers, is a crucial characteristic parameter for comparing the EC performance of the materials.[7,38] CE can be calculated according to the following formulas:

$$CE = \Delta OD/(Q/A) \quad (1)$$

$$\Delta OD = \log(T_b/T_c) \quad (2)$$

where T_b and T_c refer to the transmittances of the film in its bleached and colored states, respectively.

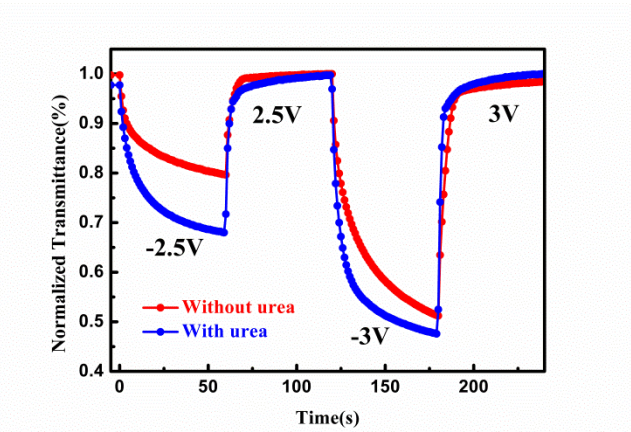

Fig. 5 In situ normalized transmittance for as-prepared films at ±2.5, ± 3V applied potentials for the optical wavelength of 632.8 nm.

Table 1 Coloration and bleaching time for as-prepared films under different applied potentials

Sample	± 2.5 V		± 3.0 V	
	color (s)	bleach (s)	color (s)	bleach (s)
With urea	31	9	21	8
Without urea	37	7.5	36	8

The CE values for each of the two samples (with urea and without urea) at the two different applied potentials (-2.5V and -3.0V) are illustrated in Fig. 6. It was evident the films exhibited higher coloration efficiency at an applied potential of -2.5 V. Fig. 6(a) shows plots of the in situ OD versus intercalation charge density at a coloration potential of -2.5 V and at a wavelength of 632.8 nm. The CE of the electrode prepared with urea is calculated to be 105.7 cm^2C^{-1}, which is higher than that of the electrode prepared without urea and some earlier reports.[9] The high coloration efficiency of the electrode prepared with urea is mainly correlated with its 2D nanosheets structure. While the applied potential increased, the overall EC efficiency of the electrode is potentially reduced. This is due to the fact that

additional energy is required to initiate the intercalation phenomenon for inducing the EC effect as the optical modulation approached saturation.[37]

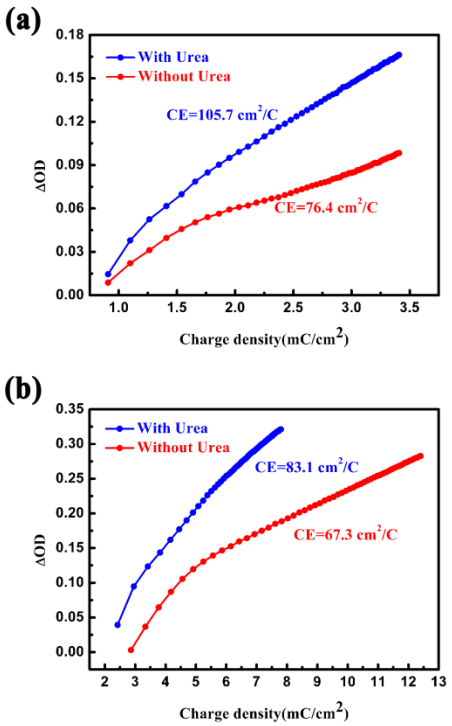

Fig. 6 Coloration efficiency of as-prepared $WO_3 \cdot 0.33H_2O$ electrode under CA at (a) ±2.5 and (b) ±3 V applied potential for the optical wavelength of 632.8 nm.

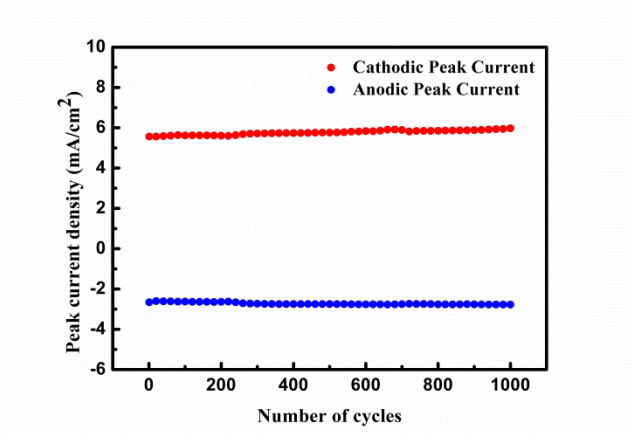

Fig. 7 Peak current evolution of the electrode prepared with urea during the step chronoamperometric cycles.

Electrochemical stability is another essential parameter for EC materials. The electrochemical stability was characterized by chronoamperometry using square potentials (between - 1.0 and 1.0 V) via a three-electrode configuration in 1 M $LiClO_4$-PC electrolyte solution, employing the as-prepared electrode as working electrode and a Pt wire (0.5 mm diameter) as the counter electrode together with an Ag/AgCl (3 M KCl) reference electrode. The peak current density of each cycle is recorded in Fig. 7. The peak current densities are almost a constant value during 1000 cycles, indicating the high stability of the as-prepared film.

Conclusions

In summary, $WO_3 \cdot 0.33H_2O$ nanosheet films have been successfully constructed on the FTO glass substrates. Systematic investigations of the influence of seed layer and urea on the morphologies and structures of the as-synthesized films have been carried out. It was found that flower-like nanorod bundles were constructed on the substrate without seed layers. Under the assistance of seed layer, uniform thin film was formed and nanorod bundles were transformed into 2D nanosheets. And the nanosheets of the uniform film will be increased after adding urea. The $WO_3 \cdot 0.33H_2O$ nanosheet film prepared with SL and urea exhibits efficient electrochromic performance, which possess promising implications for potential applications in energy-saving smart windows and displays.

Experimental Section

Preparation of seed layer

All solvents and chemicals were of analytical grade and were used without further purification. The seed layer coated FTO glass was prepared via a sol-gel method. WO_3 seed layer was deposited on an FTO coated glass substrate (cleaned sequentially using acetone, ethanol, and deionized water) by spin-coating a seed solution, followed by annealing at 400 ^oC for 1 h. The SEM images of seed layer and bare FTO glass are shown in Fig. S5. The seed solution was made by adding a 3 M HCl solution to a 0.2 M $Na_2WO_4 \cdot 2H_2O$ aqueous solution until no more precipitate was formed, and then dissolving the precipitate with 30 wt% H_2O_2.

Preparation of precursor and hydrothermal treatment

The precursor solution for hydrothermal use was prepared by dissolving H_2WO_4 (5 g) in 30 wt% H_2O_2 (60 mL), while heating at 95 ^oC with stirring. The resulting clear solution was diluted using de-ionized water to 200 mL, giving a concentration of 0.1 M. The $WO_3 \cdot 0.33H_2O$ nanosheet films were grown using an H_2WO_4 (0.1 M, 10.5 mL) solution, with HCl (3 M, 3.5 mL), de-ionized water (28 mL), and urea (1.2 mM) added to absolute ethanol (14 mL). The mixture was transferred to a 70 mL Teflon-lined stainless-steel autoclave, containing a vertically oriented FTO-coated glass (with SL, without SL); the autoclave was then sealed and maintained at 120 ^oC for 2 h. After synthesis, the substrate was rinsed with absolute ethanol and de-ionized water, and dried at room temperature.

Characterization

The morphology of the electrode was observed via a S-4800 field-emission scanning electron microscope (Hitachi, Tokyo, Japan) operated at 5 kV. TEM images and HRTEM images were obtained using a JEM 2100 F (JEOL, Tokyo, Japan) operating at 200 kV. The as-prepared electrodes were investigated using an powder X-ray diffraction technique (XRD, D/max 2550 V, Rigaku, Tokyo, Japan) with Cu Kα (λ= 1.5406A°) radiation at 40 kV and 300 mA. The transmittance spectra and the coloration/bleaching time of the electrodes were measured by

Lambda 950 (Perkin Elmer, Waltham, MA, USA). Electrochemical measurements were carried out on the CHI760D (Shanghai Chenhua Instruments, China) electrochemical workstation.

Acknowledgements

We gratefully acknowledge the financial support by Natural Science Foundation of China (No. 51172042 and No. 61376009), Specialized Research Fund for the Doctoral Program of Higher Education (20110075130001), Science and Technology Commission of Shanghai Municipality (12nm0503900, 13JC1400200), the Program for Professor of Special Appointment (Eastern Scholar) at Shanghai Institutions of Higher Learning, Innovative Research Team in University (IRT1221) and the Program of Introducing Talents of Discipline to Universities (No.111-2-04). The project was funded by State Key Laboratory for Modification of Chemical Fibers and Polymer Materials, Donghua University (LK1221).

Notes and references

[a] *State Key Laboratory for Modification of Chemical Fibers and Polymer Materials, College of Materials Science and Engineering, Donghua University, Shanghai 201620, P. R. China. E-mail: wanghz@dhu.edu.cn; Fax: +86-021-67792855; Tel: +86-021-67792881*
[b] *School of Urban Development and Environmental Engineering, Shanghai Second Polytechnic University, Shanghai 201209, P. R. China*
[c] *Engineering Research Center of Advanced Glasses Manufacturing Technology, Ministry of Education, College of Materials Science and Engineering, Donghua University, Shanghai 201620, P. R. China. E-mail: yaogang_li@dhu.edu.cn; Fax: +86-021-67792855; Tel: +86-021-67792526*
[d] *College of Chemistry, Chemical Engineering and Biotechnology, Donghua University, Shanghai 201620, China*

† Electronic Supplementary Information (ESI) available: [details of any supplementary information available should be included here]. See DOI: 10.1039/b000000x/

‡ Footnotes should appear here. These might include comments relevant to but not central to the matter under discussion, limited experimental and spectral data, and crystallographic data.

1 J. Liu, J. Zheng, J. Wang, J. Xu, H. Li and S. Yu, *Nano Lett.*, 2013, **13**, 3589.
2 Z. Jiao, J. Wang, L. Ke, X. W. Sun and H. V. Demir, *ACS Appl. Mater. Interfaces*, 2011, **3**, 229.
3 J. Li, Y. Qin, C. Jin, Y. Li, D. Shi, L. Schmidt-Mende, L. Gan and J. Yang, *Nanoscale*, 2013, **5**, 5009.
4 S. Vallejos, P. Umek, T. Stoycheva, F. Annanouch, E. Llobet, X. Correig, P. De Marco, C. Bittencour and C. Blackman, *Adv. Funct. Mater.*, 2013, **23**, 1313.
5 D. Chandra, K. Saito, T. Yui and M. Yagi, *Angew. Chem. Int. Ed.*, 2013, **52**, 12606.
6 H. Zheng, Y. Tachibana and K. Kalantar-zadeh, *Langmuir*, 2010, **26**, 19148.
7 H. Li, G. Shi, H. Wang, Q. Zhang and Y. Li, *J. Mater. Chem. A*, 2014, **2**, 11305.
8 D. Ma, H. Wang, Q. Zhang and Y. Li, *J. Mater. Chem.*, 2012, **22**, 16633.
9 D. Ma, G. Shi, H. Wang, Q. Zhang and Y. Li, *J. Mater. Chem. A*, 2013, **1**, 684.
10 H. Zheng, J. Z. Ou, M. S. Strano, R. B. Kaner, A. Mitchell and K. Kalantar-zadeh, *Adv. Funct. Mater.*, 2011, **21**, 2175.
11 G. Cai, J. Tu, D. Zhou, L. Li, J. Zhang, X. Wang and C. Gu, *CrystEngComm*, 2014, **16**, 6866.
12 C. Fu, J. C, Foo and P. S. Lee, *Electrochimica Acta*, 2014, **117**, 139.
13 M. Deepa, R. Sharma, A. Basu and S. A. Agnihotry, *Electrochim. Acta*, 2005, **50**, 3545.
14 A. I. Inamdar, Y. S. Kim, B. U. Jang, H. Im, W. Jung, D. Y. Kim and H. Kim, *Thin Solid Films*, 2012, **520**, 5367.
15 Y. C. Her and C. C. Chang, *CrystEngComm*, 2014, **16**, 5379.
16 C. Li, C. Engtrakul, R. C. Tenent, C. A. Wolden, *Sol. Energy Mater. Sol. Cells*, 2015, **132**, 6.
17 S. H. Lee, R. Deshpande, P. A. Parilla, K. M. Jones, B. To, A. H. Mahan and A. C. Dillon, *Adv. Mater.*, 2006, **18**, 763.
18 M. V. Limaye, J. S. Chen, S. B. Singh, Y. C. Shao, Y. F. Wang, C. W. Pao, H. M. Tsai, J. F. Lee, H. J. Lin, J. W. Chiou, M. C. Yang, W. T. Wu, J. S. Chen, J. J. Wu, M. H. Tsai and W. F. Pong, *RSC Adv.*, 2014, **4**, 5036.
19 L. Yang, D. Ge, J. Zhao, Y. Ding, X. Kong and Y. Li, *Sol. Energy Mater. Sol. Cells*, 2012, **100**, 251.
20 X. Yang, G. Zhu, S. Wang, R. Zhang, L. Lin, W. Wu and Z. L. Wang, *Energy Environ. Sci.*, 2012, **5**, 9462.
21 J. Z. Ou, S. Balendhran, M. R. Field, D. G. McCulloch, A. S. Zoolfakar, R. A. Rani, S. Zhuiykov, A. P. O'Mullane and K. Kalantar-zadeh, *Nanoscale*, 2012, **4**, 5980.
22 J. Y. Zheng, G. Song, C. W. Kim and Y. S. Kang, *Nanoscale*, 2013, **5**, 5279.
23 J. Zhang, J. Tu, X. Xia, X. Wang and C. Gu, *J. Mater. Chem.*, 2011, **21**, 5492.
24 M. Trapatsel, D. Vernardou, P. Tzanetakis and E. Spanakis, *ACS Appl. Mater. Interfaces*, 2011, **3**, 2726.
25 D. Vernardou, H. Drosos, E. Spanakis, E. Koudoumas, C. Savvakis and N. Katsarakis, *J. Mater. Chem.*, 2011, **21**, 513.
26 S. Balendhran, J. Z. Ou, M. Bhaskaran, S. Sriram, S. Ippolito, Z. Vasic, E. Kats, S. Bhargava, S. Zhuiykov and K. Kalantar-zadeh, *Nanoscale*, 2012, **4**, 461.
27 S. Balendhran, S. Walia, M. Alsaif, E. P. Nguyen, J. Z. Ou, S. Zhuiykov, S. Sriram, M. Bhaskaran and K. Kalantar-zadeh, *ACS Nano*, 2013, **7**, 9753.
28 L. Liang, J. Zhang, Y. Zhou, J. Xie, X. Zhang, M. Guan, B. Pan and Y. Xie, *Sci. Rep.*, 2013, **3**, 1936.
29 J. Ma, J. Zhang, S. Wang, T. Wang, J. Lian, X. Duan and W. Zheng, *J. Phys. Chem. C*, 2011, **115**, 18157.
30 M. R. Waller, T. K. Townsend, J. Zhao, E. M. Sabio, R. L. Chamousis, N. D. Browning and F. E. Osterloh, *Chem. Mater.*, 2012, **24**, 698.
31 K. Kalantar-zadeh, A. Vijayaraghavan, M. H. Ham, H. Zheng, M. Breedon and M. S. Strano, *Chem. Mater.*, 2010, **22**, 5560.
32 L. Peng, X. Peng, B. Liu, C. Wu, Y. Xie and G. Yu, *Nano Lett.*, 2013, **13**, 2151.
33 S. H. Ko, D. Lee, H. W. Kang, K. H. Nam, J. Y. Yeo, S. J. Hong, C. P. Grigoropoulos and H. J. Sung, *Nano Lett.*, 2011, **11**, 666.
34 J. Song and S. Lim, *J. Phys. Chem. C*, 2007, **111**, 596.
35 Z. G. Zhao and M. Miyauchi, *J. Phys. Chem. C*, 2009, **113**, 6539.
36 D. D. Yao, R. A. Rani, A. P. O'Mullane, K. Kalantar-zadeh and J. Z. Ou, *J. Phys. Chem. C*, 2014, **118**, 10867.
37 D. D. Yao, R. A. Rani, A. P. O'Mullane, K. Kalantar-zadeh and J. Z. Ou, *J. Phys. Chem. C*, 2014, **118**, 476.
38 J. Wang, E. Khoo, P. S. Lee and J. Ma, *J. Phys. Chem. C*, 2008, **112**, 14306.
39 Z. Jiao, X. W. Sun, J. Wang, L. Ke and H. V. Demir, *J. Phys. D: Appl. Phys.*, 2010, **43**, 285501.

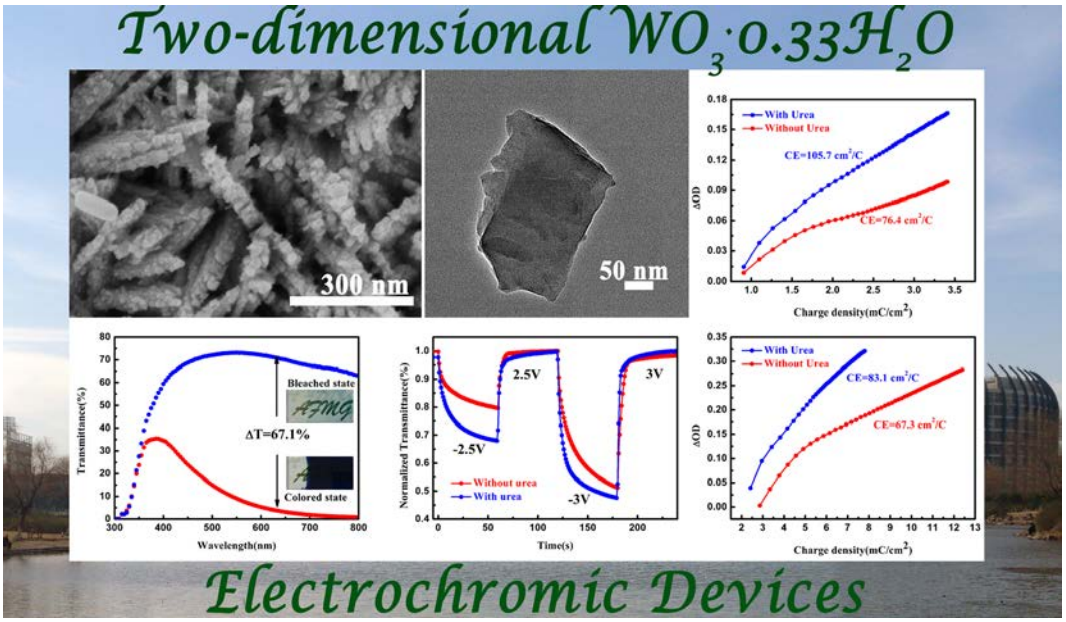

Two-dimensional WO_3 (hydrate) nanosheets, with high surface ratio and permeable channels, could be a promising building block for constructing EC electrode.